Biophysical Journal
Article

Biophysical Society

Comparative Study of the Condensing Effects of Ergosterol and Cholesterol

Wei-Chin Hung,[1] Ming-Tao Lee,[2,3] Hsien Chung,[1] Yi-Ting Sun,[2,4] Hsiung Chen,[2] Nicholas E. Charron,[5] and Huey W. Huang[5,*]

[1]Department of Physics, Republic of China Military Academy, Fengshan, Kaohsiung, Taiwan; [2]National Synchrotron Radiation Research Center, Hsinchu, Taiwan; [3]Department of Physics, National Central University, Jhongli, Taiwan; [4]Institute of Molecular Medicine, National Tsing Hua University, Hsinchu, Taiwan; and [5]Department of Physics and Astronomy, Rice University, Houston, Texas

ABSTRACT Cholesterol, due to its condensing effect, is considered an important regulator of membrane thickness. Other sterols, due to their structural similarities to cholesterol, are often assumed to have a universal effect on membrane properties similar to the condensing effect of cholesterol, albeit possibly to different degrees. We used x-ray diffraction to investigate this assumption. By the combination of lamellar diffraction and grazing-angle scattering, we measured the membrane thickness and the tilt-angle distribution of the lipid's hydrocarbon chains. This method is sensitive to phase separation, which is important for examining the miscibility of sterols and phospholipids. Mixtures of ergosterol or cholesterol with dimyristoylphosphatidylcholine, palmitoyloleoylphosphatidylcholine, and dioleoylphosphatidylcholine were systematically studied. We found that mixing ergosterol with phospholipids into a single phase became increasingly difficult with higher sterol concentrations and also with higher concentrations of unsaturated lipid chains. The only condensing effect of ergosterol was found in dimyristoylphosphatidylcholine, although the effect was less than one-third of the effect of cholesterol. Unlike cholesterol, ergosterol could not maintain a fixed electron density profile of the surrounding lipids independent of hydration. In dioleoylphosphatidylcholine and palmitoyloleoylphosphatidylcholine, ergosterol made the membranes thinner, opposite to the effect of cholesterol. In all cases, the tilt-angle variation of the chain diffraction was consistent with the membrane thickness changes measured by lamellar diffraction, i.e., a thickening was always associated with a reduction of chain tilt angles. Our findings do not support the notion that different sterols have a universal behavior that differs only in degree.

INTRODUCTION

A biological membrane is conceptualized as a system in which membrane proteins are hydrophobically matched to the equilibrium thickness of the lipid bilayer (1–3). Cholesterol, due to its condensing effect, has been suggested to be a major regulator of membrane thickness (1–3). The condensing effect was first discovered in monolayers (4,5), in which the area per phospholipid was found to decrease in the presence of cholesterol. Extensive studies of cholesterol-phospholipid mixtures in monolayers gave rise to the idea that cholesterol forms complexes with phospholipids (6–8). The corresponding effect in bilayers is that the inclusion of cholesterol increases the thickness of the phospholipid bilayer (9,10). In their pioneering work with x-ray diffraction on mixed bilayers of egg lecithin and cholesterol (9), Levine and Wilkins showed that cholesterol had the effect of reducing the distribution of the lipid-chain orientation to smaller tilt angles. Consistent with this effect, cholesterol increased the phosphate-to-phosphate distance across the bilayer (9). Since that study, the membrane-thickening effect of cholesterol on other phospholipids has been measured by many investigators (10–15). In our previous study (16), we showed that the condensing effect of cholesterol extended to the phospholipids not directly complexed with cholesterol; this might explain why the electron density profile of cholesterol-containing lipids becomes invariant with hydration (16).

Other sterols found in membranes have not been studied as extensively as cholesterol. Nevertheless, because of their chemical similarities to cholesterol, they are often considered the structural equivalents of cholesterol and are thought to play similar roles (17,18). Ergosterol, the major sterol found in the plasma membranes of yeast and other fungi (19), differs from cholesterol in having an additional double bond in a ring of the steroid nucleus and a double bond and

Submitted February 5, 2016, and accepted for publication April 5, 2016.

*Correspondence: hwhuang@rice.edu

Wei-Chin Hung and Ming-Tao Lee contributed equally to this work.

Editor: Georg Pabst.

http://dx.doi.org/10.1016/j.bpj.2016.04.003

an extra methyl group in the alkyl side chain (20) (see Fig. S1 in the Supporting Material). A good number of experimental as well as molecular-dynamics investigations have been carried out on ergosterol-phospholipid systems (21–23). However, many of the results of these studies are not in agreement with one another, in particular on the condensing effect of ergosterol (24).

The majority of past studies concentrated on saturated-chain phospholipids 14:0 phosphatidylcholine (PC) (dimyristoylphosphatidylcholine (DMPC)) and 16:0 PC (dipalmitoylphosphatidylcholine (DPPC)). Two independent simulations (21,22) showed that the condensing effect on DMPC and DPPC by ergosterol was stronger than the effect by cholesterol. Several NMR studies have reported that ergosterol was more effective than cholesterol in ordering the hydrocarbon chains of liquid crystalline DMPC (25,26) and DPPC (27) up to 30 mol % sterol concentrations. However, at sterol concentrations of 40 mol %, ergosterol was less effective than cholesterol in increasing the chain order in DPPC (22). A Fourier-transform infrared study (28) found that ergosterol at 28 mol % had a higher condensing effect on the fluid phase of DPPC than did cholesterol. Finally, a small-angle neutron scattering study (15) of DMPC containing 20 and 47 mol % sterol reported that ergosterol and cholesterol produced similar membrane thickness increases.

Two lipid systems including unsaturated chains, i.e., egg lecithin and 16:0–18:1 PC (palmitoyloleoylphosphatidylcholine (POPC)), have also been studied. A spin-label electron paramagnetic resonance study (29) found that the effect of ergosterol depended strongly on the sterol concentration, ordering or disordering the egg lecithin chains below or above 15 mol %, respectively. NMR studies found that cholesterol was more effective than ergosterol in ordering the hydrocarbon chains of POPC (25,26). Adding ergosterol to a concentration of 25 mol % increased POPC chain ordering, but further addition of ergosterol had a smaller effect on chain order (25,26), in contrast to the effect of cholesterol on POPC, where the effect on chain order was linearly proportional to the sterol concentration at least to 40 mol % (30). Although these results were not mutually consistent on the sterol concentration dependence, in general, the condensing effects of ergosterol and cholesterol were seen as comparable.

As demonstrated by Levine and Wilkins (9), x-ray diffraction directly measures the thickness of lipid bilayers and their associated chain tilt-angle distributions. We used this method to compare the effects of ergosterol and cholesterol on one phospholipid with fully saturated chains (DMPC), one with two monounsaturated chains (18:1 (Δ9-*Cis*) PC or dioleoylphosphatidylcholine (DOPC)), and one with a saturated and a monounsaturated chain (POPC). The results were not what we expected based on the results reported in the publications cited above. First, we found that mixing ergosterol with phospholipids was increasingly difficult with the increasing content of unsaturated chains; this is in contrast to cholesterol, which has no difficulty mixing with any phospholipid (16). Second, the thickening effect of ergosterol on DMPC is less than a third of the effect of cholesterol. Third, and most surprising, ergosterol actually slightly thins POPC and DOPC bilayers, opposite to the significant thickening effect of cholesterol on all lipids. These effects on the membrane thickness by both cholesterol and ergosterol are in accordance with the associated chain tilt distributions. Thus, our results contradict the common expectation that different sterols exhibit a universal behavior that differs only in degree (17). We found that ergosterol has no condensing effect similar to that of cholesterol, except for a weak effect on fully saturated lipids.

MATERIALS AND METHODS

Materials

Lipids 14:0 PC (DMPC), 18:1 (Δ9-*Cis*) PC (DOPC), and 16:0–18:1 PC (POPC) were purchased from Avanti Polar Lipids (Alabaster, AL). Cholesterol and ergosterol were purchased from Sigma-Aldrich (St. Louis, MO). All other reagents were from Sigma-Aldrich.

Sample preparation

Lipids and sterols were dissolved in chloroform (1 mg in 40 μL) and mixed according to the chosen ratios. The solvent was evaporated in an oven set at 40°C. The mixtures were redissolved in 1:1 chloroform and methanol at 1 mg/20 μL. The mixtures were subject to vortex mixing for ~30 min. (This solvent mixture spreads the lipid more evenly on a (cleaned) glass surface (31). For a silicon wafer substrate, we used 1:1 chloroform and trifluoroethanol (TFE) (31).) Using a micropipette or a Hamilton syringe, 20 μL of the mixture was twice spread evenly over 18 × 18 mm^2 of a substrate (thus, each sample was 2 mg). After the solvent evaporated, the sample was kept in 100% relative humidity (RH) at 40°C overnight and used within 24 h of the initial mixing. More details of sample preparation are available in previous publications (32,33).

Lamellar diffraction

For x-ray lamellar diffraction measurement, the sample was kept in a thermally insulated chamber ($\pm$0.1°C) that was equipped with mylar windows for x-ray passage. The chamber also enclosed a temperature-controlled water source for the humidity control. The relative humidity was measured by a hygrometer (Rotronic Instrument, Huntington, NY) that was calibrated using saturated salts. The details of the sample chamber have been described previously (32,34).

The laboratory diffractometer consisted of a two-circle goniometer and a Cu Kα radiation source filtered by Ni and operated at 40 kV/30 mA. The two-circle goniometer was designed for vertical ω-2θ scan, so that the sample substrate was kept nearly horizontal during the entire measurement. This allowed us to measure the lipid samples at high hydration levels without the problem of sample-running that might occur if the substrate were oriented vertically, as in a horizontal ω-2θ scan experiment. Both the incident and the diffracted x-rays were collimated by two sets of *x*-*y* slits.

As a routine procedure, we performed sample alignment before each ω-2θ scan (as described in (33,35)). A two-dimensional (ω, 2θ) scan around the second or third Bragg peak was used to check the alignment

of the ω-angle. A correctly aligned sample has the peak position exactly at $\omega = \theta$ in the (ω, 2θ) plane. Also the quality of the multilamellar sample could be assessed by this scan. A cut through the center of the peak along ω gives the conventional rocking curve. All of our samples exhibited a narrow peak with a full width at half-maximum of $\lesssim 0.1^\circ$ (Fig. S2), indicating excellent multilamellar alignment.

An attenuator was used to prevent the first-order Bragg peak from saturating the detector. Each ω-2θ scan was measured from $\theta = 0.5$–10.5° with a step size of $\Delta\theta = 0.01^\circ$, 1 s/step. Each sample was measured at several different hydration levels from ~95% to ~100% RH, for the purpose of using the swelling method to determine the phases of diffraction amplitudes (35–37) and for reaching the full hydration (32,33). The equilibrium of the sample at each humidity setting was ensured by the agreement of at least three consecutive diffraction patterns whose average was subsequently analyzed. Selected data points were measured with at least two separately prepared samples to ensure reproducibility. Each sample was measured twice to ensure that the samples were not damaged by radiation. In previous experiments we observed diffraction pattern changes when a sample was overexposed; such a sample also produced extra spots in the thin-layer chromatogram (37).

The procedure for data reduction has been described in many of our previous articles (35–37). Briefly, data reduction started with the background removal and corrections for absorption and diffraction volume. Then, the integrated peak intensities were corrected for polarization and Lorentz factors. The relative magnitude of the diffraction amplitude was the square root of the integrated intensity. The phases were determined by the swelling method (38). With their phases determined, the diffraction amplitudes were Fourier transformed to obtain the transbilayer electron density profiles. The profiles were not normalized to the absolute scale, but they gave the correct phosphate-peak-to-phosphate-peak (Ptp) distances (35).

Hydrocarbon chain diffraction

Grazing-angle scattering was performed at the beam line BL13A of the National Synchrotron Radiation Research Center (NSRRC), Hsinchu, Taiwan. The setup was similar to the one described in Yang and Huang (34). The sample was horizontal and positioned to let a beam of 12 keV, size 0.6×0.3 mm^2 incident at ~0.3° relative to the substrate. Scattering patterns were recorded on a Rayonix 165 detector (Rayonix, Evanston, IL), which was vertical, i.e., perpendicular to the plane of the sample substrate. An aluminum attenuator was used to keep strong reflection orders from saturating the detector.

Data analysis for chain diffraction

The point where the sample intercepts the incident x-ray is projected vertically onto the detector plane as the origin of the Q coordinates. The incident beam is on the y-z plane. The vertical and horizontal coordinates for a point P on the detector are P_z and P_x, respectively. Let H be the sample-to-detector distance and R the sample-to-data-point distance, and apply the definitions $\tan\gamma = P_x/H$ and $\sin\nu = P_z/R$; $\alpha =$ the angle between the incident beam and the substrate surface (the x-y plane); $\nu =$ the angle between the diffracted beam and the x-y plane; $\gamma =$ the angle between the in-plane (x-y) projection of the incident beam and the in-plane projection of the diffracted beam.

Then, the incident unit vector is $\vec{S}_o = (0, \cos\alpha, \sin\alpha)$; the scattering unit vector is $\vec{S} = (\cos\nu \times \sin\gamma, \cos\nu \times \cos\gamma, \sin\nu)$, and the momentum transfer is

$$\vec{Q} = \left(\frac{2\pi}{\lambda}\right)\left(\vec{S} - \vec{S}_o\right) = \frac{2\pi}{\lambda}(\cos\nu \times \sin\gamma, \cos\nu \times \cos\gamma - \cos\alpha, \sin\nu - \sin\alpha).$$

The chain tilt angle, ϕ, is given by $\sin\phi = (\sin\nu - \sin\alpha)/\sqrt{2(1 - \cos\upsilon\cos\gamma\cos\alpha - \sin\nu\sin\alpha)}$.

The intensity is corrected for the polarization factor $\cos^2\gamma$, and the relative absorption factor $(\sin\nu/\mu a)(1 - e^{-\mu a/\sin\nu})$, where μ is the absorption coefficient. The incident absorption, which is the same for all data points, is not corrected.

RESULTS

Miscibility of sterols and phospholipids

Multilamellar samples were prepared from the mixtures of sterol and phospholipid codissolved in chloroform. X-ray diffraction is sensitive to phase separation (39); therefore, it provides a test for miscibility. Lamellar diffraction generally produces more than one series of lamellar peaks if there is phase separation in bilayers (16,39). Undissolved cholesterol and ergosterol tend to form crystals (32), which are detectable by grazing-angle scattering. Fig. 1 shows the lamellar diffraction patterns of one POPC sample containing 29 mol % of ergosterol. After the sample was prepared at 25°C in full hydration, the lamellar diffraction pattern initially showed phase separation. The sample was then

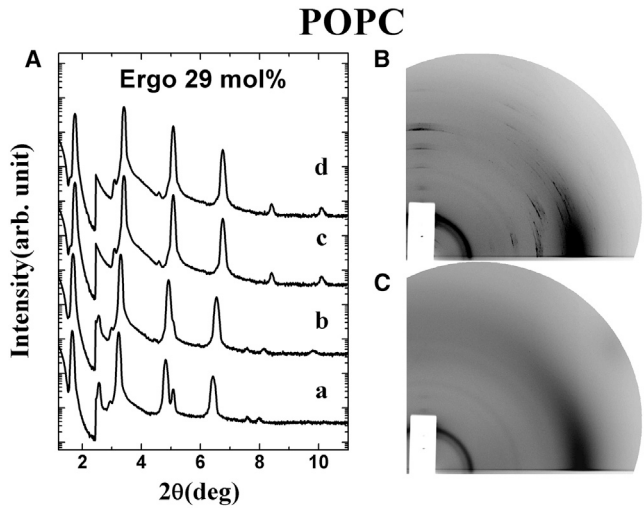

FIGURE 1 Diffraction patterns of POPC bilayers containing 29 mol % ergosterol. (*A*) Lamellar diffraction patterns. (*a*) The sample was initially made at 25°C at 100% RH, without heat incubation. The pattern contained two series of lamellar peaks at different repeat distances. (*b*) After 1.5 h of incubation at 40°C, there were still traces of two series of lamellar peaks. (*c*) After 10 h of heat incubation, the pattern had only one series of lamellar peaks. (*d*) After 18 h of heat incubation, the pattern observed in (*c*) had not changed. (*B*) Grazing-angle scattering of the sample in condition (*A* (*d*)) showed diffraction of partially oriented ergosterol crystals (sharp short arcs grouped in patches; their Q positions are shown in Fig. S3). (*C*) Grazing-angle scattering from pure POPC (that contains no crystalline diffraction), for comparison with (*B*). The small dark circles in (*B*) and (*C*) are the characteristic Kapton rings, due to several Kapton windows used at the beam-pipe opening (to keep vacuum at 10^{-3} atm) and for the sample chamber. Note that the intensity of chain diffraction is much smaller than that of lamellar diffraction. To show the chain diffraction clearly, the contrast of the charge-coupled device image was adjusted to the low-intensity range.

kept at 40°C in full hydration and measured repeatedly as a function of incubation time. The sample appeared to equilibrate into a single phase by lamellar diffraction after ~10 h of 40°C incubation. However, the grazing-angle scattering of this sample showed a diffraction signal from partially oriented ergosterol crystals that apparently were not dissolved in the lipid (Figs. 1 and S3).

The solubility limits of sterols in phospholipids are an issue that has been previously investigated (40). We did not attempt to find the solubility limit of ergosterol in multilamellar samples, because the solubility or miscibility depends on the temperature and the length of time a sample is incubated. We decided to prepare all samples the same way. All samples were incubated overnight at 40°C in full hydration and measured within 24 h after the initial mixing (the detailed procedure is described in Materials and Methods). X-ray measurements were performed at either 25° or 30°C in full hydration. The results showed very small temperature dependence from 25° to 30°C.

Each sterol-phospholipid composition was measured for lamellar diffraction by a θ-2θ scan and for lipid chain diffraction by grazing-angle scattering. We analyzed a composition only if it produced a single series of lamellar peaks and produced no sterol crystalline diffraction detectable through grazing-angle scattering. There is a noticeable difference between cholesterol and ergosterol in their miscibility with phospholipids. We found that all cholesterol-PC mixtures were in a single phase up to at least ~40 mol % of cholesterol, as was ergosterol-DMPC up to at least ~40 mol % of ergosterol. However, mixing ergosterol with POPC or DOPC became difficult at high sterol concentrations. Ergosterol-POPC mixtures were in a single phase only up to 20 mol % of ergosterol. Despite numerous trials, none of the ergosterol-POPC mixtures at 23 mol % were in a single phase. The highest ergosterol concentration in DOPC mixtures that produced a single phase was 7 mol %.

Electron density profiles of bilayers by lamellar diffraction

Examples of lamellar diffraction were shown in Fig. S4. The electron density profiles across the bilayers were constructed from the integrated diffraction peaks (Fig. S4) (16). We define the bilayer thickness as the PtP distances across the bilayer at full hydration. The results are plotted in Fig. 2, with previously published cholesterol/DMPC and cholesterol/DOPC results included (16).

Cholesterol shows a strong condensing effect on DMPC, increasing its thickness from ~36.0 Å to ~43.3 Å. Ergosterol also shows a condensing effect, but less than one-third that of cholesterol, increasing the DMPC thickness from ~36.0 Å to ~38.0 Å (Fig. 2 *A*).

Most surprisingly, ergosterol caused thinning of the POPC and DOPC bilayers, opposite to the condensing effect of cholesterol. Because of the limitation on the ergosterol concentration in DOPC, we carefully investigated the effect of ergosterol on POPC as a function of ergosterol concentrations up to 20 mol %. Fig. 2 *B* shows our data measured in three different laboratories (Republic of China Military Academy, Rice University, and the National Synchrotron Radiation Research Center) by different investigators. Each investigator used the same method to independently prepare samples. The data show that not only does ergosterol have no condensing effect on POPC, it actually causes slight thinning. Therefore, it must have (slightly) increased the molecular area of POPC, opposite to the condensing effect of cholesterol.

Ergosterol mixed uniformly with DOPC only up to 7 mol % by our method of sample preparation. DOPC containing 9 mol % of ergosterol had only one series of lamellar peaks, but its grazing-angle scattering showed a minute amount of crystalline diffraction (Fig. S5). Similar to the case with POPC, ergosterol slightly thinned the DOPC bilayers (Fig. 2 *C*).

In addition to the effects on bilayer thickness, the profiles of electron density also display the ordering effect on the lipid molecules. This is most obvious at high sterol concentrations. Fig. 3 compares the effects of cholesterol and ergosterol on the electron density profile of DMPC, which will be discussed below.

Tilt-angle distribution of chain diffraction

To understand the causes of membrane thickening or thinning, we examined the tilt-angle distribution of the chain

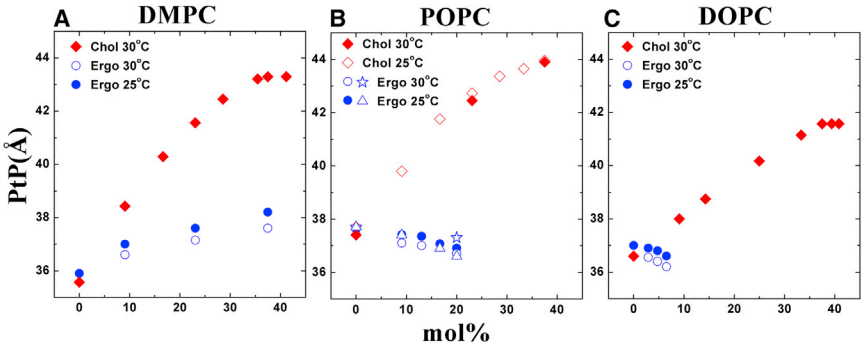

FIGURE 2 PtP distances of fully hydrated bilayers measured by lamellar diffraction. (*A*) DMPC series. (*B*) POPC series. (*C*) DOPC series. The data for cholesterol/DMPC and cholesterol/DOPC series were reproduced from (16). The data indicated by solid and open circles are from the Republic of China Military Academy, those indicated by triangles are from Rice University, and those indicated by stars are from NSRRC. The corresponding *d*-spacing for each PtP value is given in Table S1.

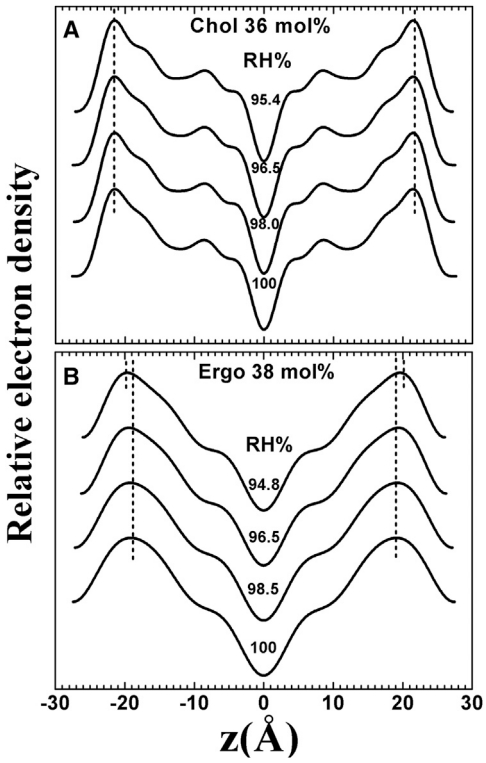

FIGURE 3 Electron density profiles of DMPC containing 36 mol % cholesterol (*A*) compared with DMPC containing 38 mol % ergosterol (*B*). The profiles of DMPC containing cholesterol are unchanged from ~95 to 100% RH, whereas the profiles for DMPC containing ergosterol noticeably vary with humidity, particularly the phosphate-peak position. The diffraction patterns for these electron density profiles are shown in Fig. S6.

diffraction by grazing-angle scattering. The hydrocarbon chains of phospholipids produce liquid paraffin-like diffraction at ~4.6 Å (9,41) (Fig. 4). Following Levine and Wilkins (9), we consider the hydrocarbon region of each bilayer as an assembly of domains, each of which consists of parallel-packed chain segments (9). Each domain independently diffracts in a plane perpendicular to the axes of the chains, which make a tilt angle, ϕ, with respect to the normal to the bilayer plane. According to this Levine-Wilkins model, the tilt-angle distribution of the radially integrated chain diffraction represents the distribution of the chain-segment domains in their tilt angles (42,43).

First, the raw data were replotted in the plane of momentum transfer components (43) Q_z versus Q_{xy} (Fig. 5 *A*) (see Materials and Methods). Here, the chain tilt angle, ϕ, is the projection angle of $\vec{Q}$ onto the plane of membrane (xy plane). Note that the detectable range of (Q_z, Q_{xy}) is limited by the diffraction geometry and the incident angle, α (44). At incident angle $\alpha = 0.3$, the detectable range includes $0^\circ \leq \phi \leq 81.8^\circ$, sufficient for the lipid systems studied here.

The diffraction intensity along a radial direction was integrated after removing the background (Fig. 5 *B*). The radially integrated intensity is proportional to the probability, P, of diffraction from a chain domain oriented at some tilt angle, ϕ, and some azimuthal angle, ψ. However, the chain orientation is independent of the azimuthal angle; therefore, the probability, P, is only a function of the tilt angle: $P(\phi)$. Assuming that the chain orientation is limited to the solid angle within one hemisphere, the integration of $P(\phi)$ over the hemisphere equals 1: $\int P(\phi) d(\cos\phi) d\psi = 1$ or $\int_0^1 P(\phi) d(\cos\phi) = 1/2\pi$. This condition is used to normalize the distribution functions $P(\phi)$ for different sterol concentrations. The normalized distribution function $P(\phi)$ is plotted on the coordinate $\cos\phi$, so that the area under each distribution represents the probability of finding the chains at the corresponding tilt angle (Fig. 6).

DISCUSSION

The model conceptualized by Levine and Wilkins for chain diffraction is not an exact theory in the fluid phase of lipids, as pointed out by Warren in his analysis of the paraffin peak (41). It would be exact if the chain domains consist of regular hexagonal packs of cylindrical chains, as, for example, in the gel phase of DMPC (39); such a model (e.g., (45)), if applied to our data, would not produce bilayer thicknesses in agreement with the measured PtP values. How to refine the model so as to quantify the relation between the chain diffraction and the bilayer thickness is still unknown. We will show that qualitatively the tilt-angle variation of the chain diffraction (Figs. 4 and 6) is consistent with the membrane thickness measured by lamellar diffraction (Fig. 2). Because our results on the condensing effect of ergosterol contradict previously published conclusions, it is important that two independent methods, i.e., the thickness measure and the chain angle distribution, both support our results.

Cholesterol increased the thickness of all phospholipids (Fig. 2), in agreement with earlier measurements (9,10,12–15,46). In DMPC, the increase was >7 Å. Ergosterol also increased the thickness of DMPC, but its effect was less than one-third of the effect of cholesterol (Fig. 2 *A*). Consistently, both cholesterol and ergosterol reduced the chain tilt, i.e., redistributed the chains in high tilt angles to low tilt angles (Fig. 6 *A*). The smaller tilt angles create a larger projection of the chain segments in the normal direction, resulting in a thicker bilayer.

Our experiment found another important difference between cholesterol and ergosterol in their interactions with DMPC. It is well known that a pure lipid bilayer changes its electron density profile and thickness with the degree of hydration over a range of RH, ~95–100% (9,46–48). However, if the bilayers contain a significant amount of cholesterol ($\gtrsim$ 9 mol %), this effect is absent (10,12,16,46,48) and the structure of the electron density profile of the bilayer becomes independent of the degree of hydration (12,16). For this reason, cholesterol is called a membrane-thickness buffer (12). Fig. 3 shows the electron

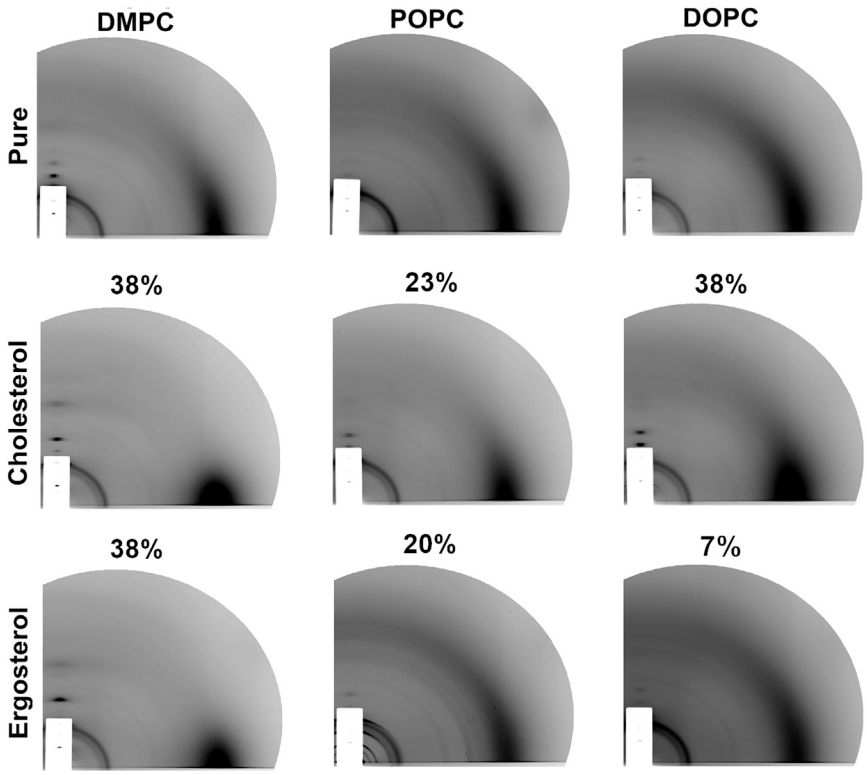

FIGURE 4 Detector images of the grazing-angle scattering patterns. Each column is for one phospholipid in pure form (*top row*), containing cholesterol at the labeled mol % (*middle row*), and containing ergosterol at the labeled mol % (*bottom row*). All samples were measured at full hydration. We show POPC containing 23% cholesterol (instead of the higher 38%) to compare with POPC containing 20% ergosterol. The center of the circular pattern is $\vec{Q} = 0$ where the meridional axis is the Q_z coordinate. An attenuator was in place to block the strong peaks. The diffuse circular patterns (strongest at the equator) are the hydrocarbon chain diffraction bands, often called the paraffin bands or paraffin peaks. The contrast of the charge-coupled device image was adjusted to the low-intensity range to enhance the chain diffraction, which also exaggerated the intensity of the Kapton rings and the reflections on the z axis.

density profiles of DMPC containing 36 mol % cholesterol compared with DMPC containing 38 mol % ergosterol. The profiles containing cholesterol are unchanged with humidity from ~95 to 100% RH, whereas the profiles for DMPC containing ergosterol noticeably vary with humidity. Furthermore, the electron density profile of DMPC containing cholesterol shows details of density variations somewhat similar to those observed for pure DMPC in the gel phase (49). In contrast, the profile for DMPC containing ergosterol is much smoother, indicating more disorder among the individual lipid molecules.

Our results show clearly that the condensing and chain-ordering effects of ergosterol on DMPC are smaller than those of cholesterol. This is contradictory to almost all previous studies, both experimental and molecular-simulation based, which found the condensing and chain-ordering effects of ergosterol on DMPC to be stronger than (or in one case comparable to) the effects of cholesterol (15,21–23,25,26).

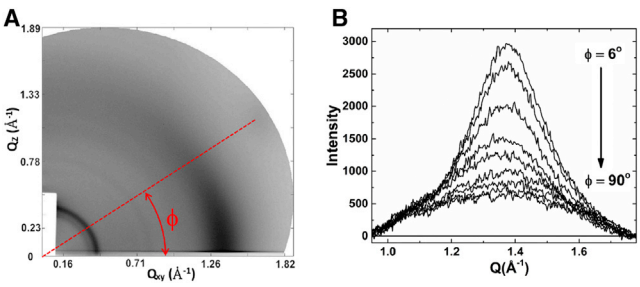

FIGURE 5 Data reduction for chain diffraction. (*A*) As an example, the chain diffraction pattern of pure POPC has been replotted in the (Q_z, Q_{xy}) plane. The red line is a radial cut at the chain tilt angle, ϕ. (*B*) The diffraction intensity along a radius in (*A*) in a series of ϕ angles, after removing the background.

The difference between ergosterol and cholesterol is much more obvious in their interactions with POPC and DOPC. Whereas cholesterol induces a strong condensing effect that thickens both POPC and DOPC bilayers, ergosterol shows no condensing effect in POPC and DOPC at all. We have systematically measured the effect of ergosterol on POPC up to 20 mol %. The POPC bilayer thickness systematically decreased, although only slightly, with ergosterol concentration (Fig. 2 *B*). This result is entirely consistent with the tilt-angle distribution of the radially integrated intensity of chain diffraction shown in Fig. 6 *B*, where cholesterol strongly reduced the chain tilt to smaller angles, but ergosterol showed no effect. The effect of ergosterol on DOPC (Figs. 2 *C* and 6 *C*) is similar to its effect on POPC, although the measurement was limited to relatively small ergosterol concentrations in DOPC.

Thus, our results show no ordering effect on the lipid chains of POPC and DOPC by ergosterol. This contradicts previous NMR studies (25,26,30), which reported that ergosterol increased the order of the phospholipid acyl chains in POPC up to 25 mol % and that beyond that level, it had a smaller ordering effect.

For our experiments, the quality of samples was an important issue. We used the combination of lamellar diffraction and grazing-angle scattering to detect possible phase

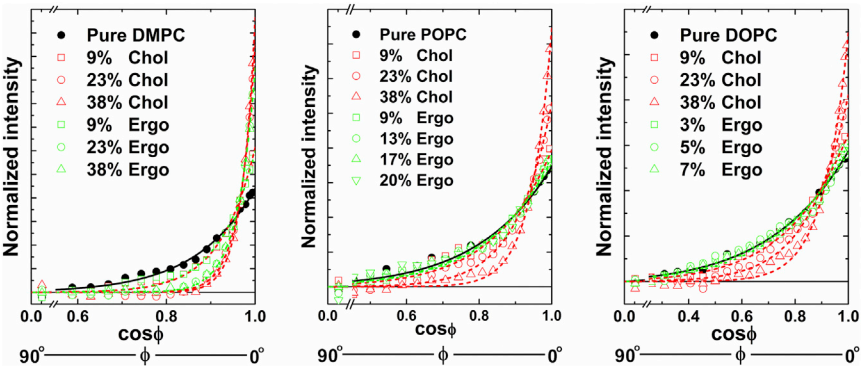

FIGURE 6 Tilt-angle variation of the normalized radially integrated intensity, $P(\phi)$. Data are represented in black for the lipid in its pure form, green for the lipid containing ergosterol, and red for the lipid containing cholesterol. Data are provided up to 38 mol % cholesterol in all lipids. Data provided for ergosterol are up to 38 mol % in DMPC, 20 mol % in POPC, and 7 mol % in DOPC.

separation in multilamellar samples. By these criteria, our sample preparation produced no single-phase, uniform samples of POPC containing ergosterol above 20 mol % and no single-phase, uniform samples of DOPC containing ergosterol above 7 mol %. In contrast, all phospholipids containing cholesterol, prepared in the same way, were in a single phase, at least up to 40 mol %. At least one previous report (25) indicated the possibility of aggregations occurring in their samples containing >25 mol % ergosterol.

Cholesterol apparently has the effect of straightening, and therefore lengthening, the lipid chains, both saturated and unsaturated. As first pointed out by Franks and Lieb (50) and discussed in detail in Hung et al. (16), this is similar to hydrophobic matching to approach the hydrophobic thickness of a pair of cholesterol molecules, very much like the phenomenon of hydrophobic matching to gramicidin channels (51). Indeed, gramicidin also renders the electron density profiles of the surrounding lipids invariant with hydration levels (48). The effect of ergosterol on DMPC, POPC, and DOPC bears no resemblance to a hydrophobic-matching effect. The interactions of ergosterol and cholesterol with lipid chains are dissimilar, particularly with unsaturated chains. This finding also suggests a focus for future studies of other sterols.

SUPPORTING MATERIAL

Six figures and one table are available at http://www.biophysj.org/biophysj/supplemental/S0006-3495(16)30152-7.

AUTHOR CONTRIBUTIONS

W.C.H., M.T.L., and H.W.H. designed the research. W.C.H., H.C., M.T.L., and N.E.C. performed lamellar diffraction and analysis. M.T.L., Y.T.S., and H.C. performed the grazing-angle scattering experiment. M.T.L. and H.W.H. analyzed chain diffraction. W.C.H., M.T.L., and H.W.H interpreted the results. N.E.C. and H.W.H. wrote the article.

ACKNOWLEDGMENTS

This work was supported by Taiwan MOST grants 104-2112-M-145-002 (to W.C.H.) and 104-2112-M-213-001 (to M.T.L.), National Institutes of Health grant GM55203, and Robert A. Welch Foundation grant C-0991 (to H.W.H.).

REFERENCES

1. Mitra, K., I. Ubarretxena-Belandia, …, D. M. Engelman. 2004. Modulation of the bilayer thickness of exocytic pathway membranes by membrane proteins rather than cholesterol. *Proc. Natl. Acad. Sci. USA.* 101:4083–4088.
2. Mouritsen, O. G., and M. Bloom. 1984. Mattress model of lipid-protein interactions in membranes. *Biophys. J.* 46:141–153.
3. Killian, J. A. 1998. Hydrophobic mismatch between proteins and lipids in membranes. *Biochim. Biophys. Acta.* 1376:401–415.
4. Leathes, J. B. 1925. Condensing effect of cholesterol on monolayers. *Lancet.* 208:853–856.
5. Radhakrishnan, A., and H. M. McConnell. 1999. Condensed complexes of cholesterol and phospholipids. *Biophys. J.* 77:1507–1517.
6. Gershfeld, N. L. 1978. Equilibrium studies of lecithin-cholesterol interactions I. Stoichiometry of lecithin-cholesterol complexes in bulk systems. *Biophys. J.* 22:469–488.
7. Subramaniam, S., and H. M. McConnell. 1987. Critical mixing in monolayer mixtures of phospholipid and cholesterol. *J. Phys. Chem.* 91:1715–1718.
8. Radhakrishnan, A., and H. M. McConnell. 1999. Cholesterol-phospholipid complexes in membranes. *J. Am. Chem. Soc.* 121:486–487.
9. Levine, Y. K., and M. H. Wilkins. 1971. Structure of oriented lipid bilayers. *Nat. New Biol.* 230:69–72.
10. Worcester, D. L., and N. P. Franks. 1976. Structural analysis of hydrated egg lecithin and cholesterol bilayers. II. Neutrol diffraction. *J. Mol. Biol.* 100:359–378.
11. McIntosh, T. J., and P. W. Holloway. 1987. Determination of the depth of bromine atoms in bilayers formed from bromolipid probes. *Biochemistry.* 26:1783–1788.
12. Franks, N. P. 1976. Structural analysis of hydrated egg lecithin and cholesterol bilayers. I. X-ray diffraction. *J. Mol. Biol.* 100:345–358.
13. Rappolt, M., M. F. Vidal, …, P. Laggner. 2003. Structural, dynamic and mechanical properties of POPC at low cholesterol concentration studied in pressure/temperature space. *Eur. Biophys. J.* 31:575–585.
14. Gallová, J., D. Uhríková, …, P. Balgavý. 2004. Bilayer thickness in unilamellar extruded 1,2-dimyristoleoyl and 1,2-dierucoyl phosphatidylcholine vesicles: SANS contrast variation study of cholesterol effect. *Colloids Surf. B Biointerfaces.* 38:11–14.
15. Pencer, J., M. P. Nieh, …, J. Katsaras. 2005. Bilayer thickness and thermal response of dimyristoylphosphatidylcholine unilamellar vesicles containing cholesterol, ergosterol and lanosterol: a small-angle neutron scattering study. *Biochim. Biophys. Acta.* 1720:84–91.
16. Hung, W. C., M. T. Lee, …, H. W. Huang. 2007. The condensing effect of cholesterol in lipid bilayers. *Biophys. J.* 92:3960–3967.

17. Henriksen, J., A. C. Rowat, …, J. H. Ipsen. 2006. Universal behavior of membranes with sterols. *Biophys. J.* 90:1639–1649.
18. Yeagle, P. L. 1993. The Membranes of Cells. Academic Press, New York.
19. Nes, W. R., and M. L. McKean. 1977. Biochemistry of Steroids and other Isopentenoids. University Park Press, Baltimore, MD.
20. Bagiński, M., A. Tempczyk, and E. Borowski. 1989. Comparative conformational analysis of cholesterol and ergosterol by molecular mechanics. *Eur. Biophys. J.* 17:159–166.
21. Czub, J., and M. Baginski. 2006. Comparative molecular dynamics study of lipid membranes containing cholesterol and ergosterol. *Biophys. J.* 90:2368–2382.
22. Cournia, Z., G. M. Ullmann, and J. C. Smith. 2007. Differential effects of cholesterol, ergosterol and lanosterol on a dipalmitoyl phosphatidylcholine membrane: a molecular dynamics simulation study. *J. Phys. Chem. B.* 111:1786–1801.
23. Smondyrev, A. M., and M. L. Berkowitz. 2001. Molecular dynamics simulation of the structure of dimyristoylphosphatidylcholine bilayers with cholesterol, ergosterol, and lanosterol. *Biophys. J.* 80:1649–1658.
24. Mannock, D. A., R. N. Lewis, and R. N. McElhaney. 2010. A calorimetric and spectroscopic comparison of the effects of ergosterol and cholesterol on the thermotropic phase behavior and organization of dipalmitoylphosphatidylcholine bilayer membranes. *Biochim. Biophys. Acta.* 1798:376–388.
25. Urbina, J. A., S. Pekerar, …, E. Oldfield. 1995. Molecular order and dynamics of phosphatidylcholine bilayer membranes in the presence of cholesterol, ergosterol and lanosterol: a comparative study using ^{2}H-, ^{13}C- and ^{31}P-NMR spectroscopy. *Biochim. Biophys. Acta.* 1238: 163–176.
26. Urbina, J. A., B. Moreno, …, E. Oldfield. 1998. A carbon-13 nuclear magnetic resonance spectroscopic study of inter-proton pair order parameters: a new approach to study order and dynamics in phospholipid membrane systems. *Biophys. J.* 75:1372–1383.
27. Hsueh, Y. W., K. Gilbert, …, J. Thewalt. 2005. The effect of ergosterol on dipalmitoylphosphatidylcholine bilayers: a deuterium NMR and calorimetric study. *Biophys. J.* 88:1799–1808.
28. Fournier, I., J. Barwicz, …, P. Tancrède. 2008. The chain conformational order of ergosterol- or cholesterol-containing DPPC bilayers as modulated by Amphotericin B: a FTIR study. *Chem. Phys. Lipids.* 151:41–50.
29. Semer, R., and E. Gelerinter. 1979. A spin label study of the effects of sterols on egg lecithin bilayers. *Chem. Phys. Lipids.* 23:201–211.
30. Hsueh, Y. W., M. T. Chen, …, J. Thewalt. 2007. Ergosterol in POPC membranes: physical properties and comparison with structurally similar sterols. *Biophys. J.* 92:1606–1615.
31. Ludtke, S., K. He, and H. Huang. 1995. Membrane thinning caused by magainin 2. *Biochemistry.* 34:16764–16769.
32. Weiss, T. M., L. Yang, …, H. W. Huang. 2002. Two states of cyclic antimicrobial peptide RTD-1 in lipid bilayers. *Biochemistry.* 41: 10070–10076.
33. Weiss, T. M., P. C. van der Wel, …, H. W. Huang. 2003. Hydrophobic mismatch between helices and lipid bilayers. *Biophys. J.* 84:379–385.
34. Yang, L., and H. W. Huang. 2003. A rhombohedral phase of lipid containing a membrane fusion intermediate structure. *Biophys. J.* 84:1808–1817.
35. Wu, Y., K. He, …, H. W. Huang. 1995. X-ray diffraction study of lipid bilayer membranes interacting with amphiphilic helical peptides: diphytanoyl phosphatidylcholine with alamethicin at low concentrations. *Biophys. J.* 68:2361–2369.
36. Chen, F. Y., W. C. Hung, and H. W. Huang. 1997. Critical swelling of phospholipid bilayers. *Phys. Rev. Lett.* 79:4026–4029.
37. Chen, F. Y., M. T. Lee, and H. W. Huang. 2003. Evidence for membrane thinning effect as the mechanism for peptide-induced pore formation. *Biophys. J.* 84:3751–3758.
38. Blaurock, A. E. 1971. Structure of the nerve myelin membrane: proof of the low-resolution profile. *J. Mol. Biol.* 56:35–52.
39. Huang, J., J. T. Buboltz, and G. W. Feigenson. 1999. Maximum solubility of cholesterol in phosphatidylcholine and phosphatidylethanolamine bilayers. *Biochim. Biophys. Acta.* 1417:89–100.
40. Stevens, M. M., A. R. Honerkamp-Smith, and S. L. Keller. 2010. Solubility limits of cholesterol, lanosterol, ergosterol, stigmasterol, and β-sitosterol in electroformed lipid vesicles. *Soft Matter.* 6:5882–5890.
41. Warren, B. E. 1933. X-ray diffraction in long chain liquids. *Phys. Rev.* 44:969–973.
42. Spaar, A., and T. Salditt. 2003. Short range order of hydrocarbon chains in fluid phospholipid bilayers studied by x-ray diffraction from highly oriented membranes. *Biophys. J.* 85:1576–1584.
43. Weinhausen, B., S. Aeffner, …, T. Salditt. 2012. Acyl-chain correlation in membrane fusion intermediates: x-ray diffraction from the rhombohedral lipid phase. *Biophys. J.* 102:2121–2129.
44. Yang, L., T. A. Harroun, …, H. W. Huang. 1998. Neutron off-plane scattering of aligned membranes. I. Method of measurement. *Biophys. J.* 75:641–645.
45. Mills, T. T., G. E. Toombes, …, J. F. Nagle. 2008. Order parameters and areas in fluid-phase oriented lipid membranes using wide angle x-ray scattering. *Biophys. J.* 95:669–681.
46. McIntosh, T. J. 1978. The effect of cholesterol on the structure of phosphatidylcholine bilayers. *Biochim. Biophys. Acta.* 513:43–58.
47. Torbet, J., and M. H. Wilkins. 1976. X-ray diffraction studies of lecithin bilayers. *J. Theor. Biol.* 62:447–458.
48. Olah, G. A., H. W. Huang, …, Y. L. Wu. 1991. Location of ion-binding sites in the gramicidin channel by x-ray diffraction. *J. Mol. Biol.* 218:847–858.
49. Smith, G. S., E. B. Sirota, …, N. A. Clark. 1990. X ray structural studies of freely suspended ordered hydrated DMPC multimembrane films. *J. Chem. Phys.* 92:4519–4529.
50. Franks, N. P., and W. R. Lieb. 1979. The structure of lipid bilayers and the effects of general anaesthetics. An x-ray and neutron diffraction study. *J. Mol. Biol.* 133:469–500.
51. Harroun, T. A., W. T. Heller, …, H. W. Huang. 1999. Experimental evidence for hydrophobic matching and membrane-mediated interactions in lipid bilayers containing gramicidin. *Biophys. J.* 76:937–945.

Biophysical Journal, Volume *110*

Supplemental Information

Comparative Study of the Condensing Effects of Ergosterol and Cholesterol

Wei-Chin Hung, Ming-Tao Lee, Hsien Chung, Yi-Ting Sun, Hsiung Chen, Nicholas E. Charron, and Huey W. Huang

Biophysical Journal

Supporting Material

Supplemental Information

Comparative Study of the Condensing Effects of Ergosterol and Cholesterol

Wei-Chin Hung, Ming-Tao Lee, Hsien Chung, Yi-Ting Sun, Hsiung Chen,
Nicholas E. Charron, Huey W. Huang*

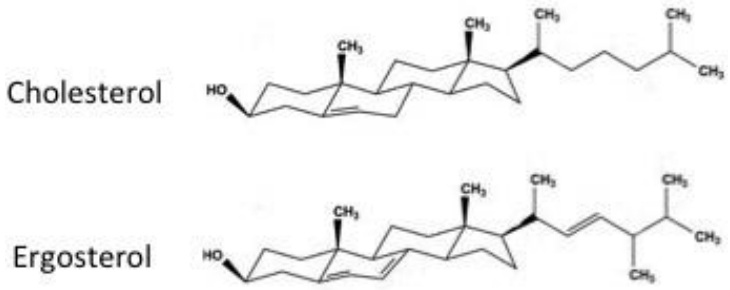

Fig. S1. The chemical structures of cholesterol and ergosterol.

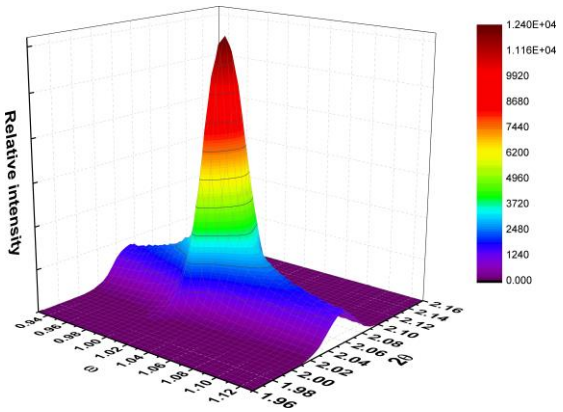

Fig. S2. As a routine procedure, we performed a two-dimensional (ω, 2θ) scan around a lamellar peak for each sample prior to the ω-2θ scan [see details in refs. 33, 35]. This is for sample alignment and for inspecting the sample quality. A correctly aligned sample has the peak position exactly at $\omega = \theta$ in the (ω, 2θ) plane. A cut through the center of the peak along ω gives the conventional rocking curve. Shown as an example is the sample DMPC containing 38 mol% ergosterol (Fig. 3B). All of our samples exhibited a narrow peak with a FWHM width $\lesssim$ 0.1 deg.

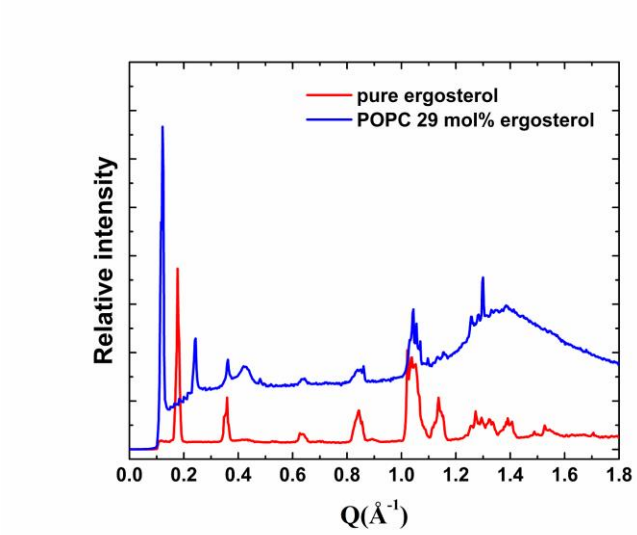

Fig. S3. The Q positions of the crystalline diffraction peaks (blue) in Fig. 1B compared with the diffraction peaks from pure ergosterol crystals (red)

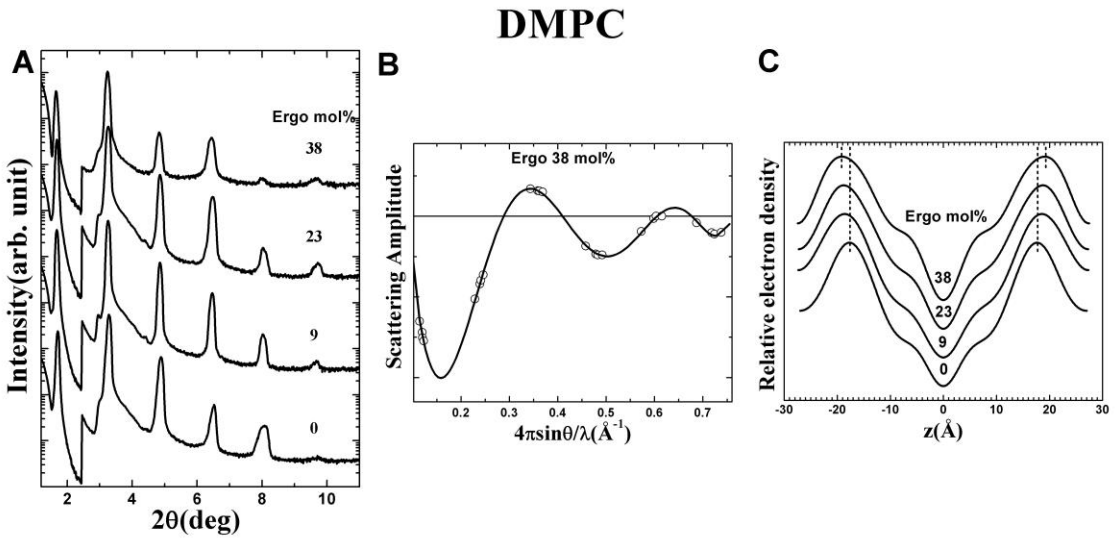

Fig. S4. Examples of lamellar diffraction analysis [see (16)]: ergosterol/DMPC series . A. Raw data of lamellar diffraction. B. Phase determination by the swelling method for an ergosterol/DMPC composition. C. Electron density profiles constructed from the lamellar diffraction series.

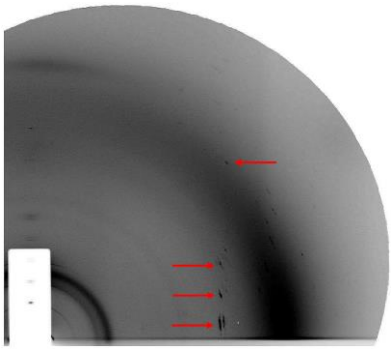

Fig. S5. Grazing-angle scattering of DOPC containing 9 mol% of ergosterol. Note diffraction of partially oriented crystal powders (indicated by arrows).

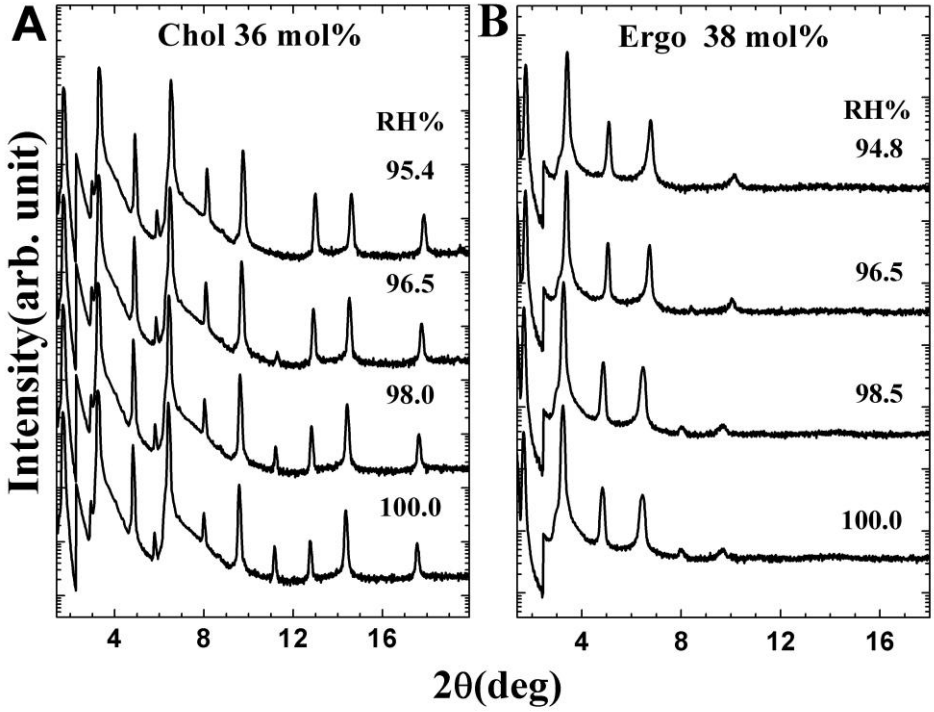

Fig. S6. The diffraction patterns of DMPC containing 36 mol% cholesterol (A) and DMPC containing 38 mol% ergosterol (B) that produced the electron density profiles displayed in Fig. 3.

DMPC								
	Chol 30°C		Chol 25°C		Ergo 30°C		Ergo 25°C	
mol%	PtP(Å)	D(Å)	PtP(Å)	D(Å)	PtP(Å)	D(Å)	PtP(Å)	D(Å)
0	35.5	51.6	35.9	51.8	35.5	51.6	35.9	51.8
9	38.4	53.4			36.6	53.2	37.1	53.4
17	40.3	55.7						
23	41.6	55.7			37.2	53.5	37.6	53.6
29	42.5	55.8						
35	43.2	55.8						
38	43.3	55.9			37.7	54.4	38.2	54.5
41	43.3	55.9						
POPC								
0	37.4	52.8	37.7	52.7	37.4	52.8	37.7	52.7
9			39.8	55.7	37.1	53.1	37.4	53.3
13					37.0	52.9	37.3	52.9
17			41.8	55.5			37.1	52.7
20					36.7	52.7		
23	42.5	55.6	42.7	55.9				
29			43.4	56.1				
33			43.6	57.2				
38	44.0	57.5	44.1	57.7				
DOPC								
0	36.6	52.6	37.0	53.0	36.6	52.6	37.0	53.0
3					36.5	52.7	36.9	52.9
5					36.4	52.6	36.8	52.9
7					36.2	52.5	36.6	52.8
9	38.0	52.6						
14	38.8	52.7						
25	40.2	52.7						
33	41.2	52.8						
38	41.6	52.6						
39	41.6	52.7						
41	41.6	52.6						

Table S1. The corresponding d-spacings (D in the table) for the PtP values shown in Fig 2.